Revista Mexicana de Física **42**, *No. 6 (1996) 1070–1086*

Classical trajectories in Coulomb three body systems

FERNANDO PÉREZ* AND JORGE MAHECHA†
Departamento de Física, Universidad de Antioquia
Apartado aéreo 1226, Medellín, Colombia

Recibido el 18 de abril de 1996; aceptado el 22 de mayo de 1996

ABSTRACT. A computer program for calculating orbits and Poincaré sections in the classical Coulomb three body problem with arbitrary masses and charges in three dimensional space is presented. The regularization procedure necessary to obtain a reliable numerical integration of the equations of motion is sketched. Different configurations of the helium atom and the positronium negative ion (Ps^-), obtained with the program, are analyzed.

RESUMEN. Se presenta un programa de computadora para calcular órbitas y secciones de Poincaré en el problema Coulombiano clásico de los tres cuerpos, con masas y cargas arbitrarias. Se esboza el procedimiento de regularización necesario para obtener una integración numérica confiable de las ecuaciones de movimiento. Se analizan diferentes configuraciones obtenidas con el programa para el átomo de helio y el ion negativo de positronio (Ps^-).

PACS: 31.10.+z; 31.90.+s; 33.10.Eb

1. INTRODUCTION

The three body problem (TBP), stated as the study of the evolution of three point-like particles whose interaction is gravitational or electrostatic in an otherwise empty space, is a long time classical and perhaps one of the most frequently tackled challenges of mathematical physics.

However, the non-integrable character of the problem renders useless the attempt of finding a function of time describing the three particles' evolution after starting from arbitrary initial conditions. This forces the adoption of other strategies, mainly:

a) A qualitative approach where questions of topological character concerning the solutions are addressed.
b) Attempts to obtain analytical solutions to cases in which certain symmetries (geometrical, dynamical or both) permit simplifications to be performed.
c) Numerical solutions to cases ranging from restricted ones such as those mentioned in (b) to the most general one where all parameters can be varied.

In this work, we shall present a computer program developed in the language C++, which calculates orbits for the electrostatic TBP with arbitrary masses, charges, and initial conditions in three dimensional space.

* E-mail: fperez@pegasus.udea.edu.co.
† E-mail: mahecha@fisica.udea.edu.co.

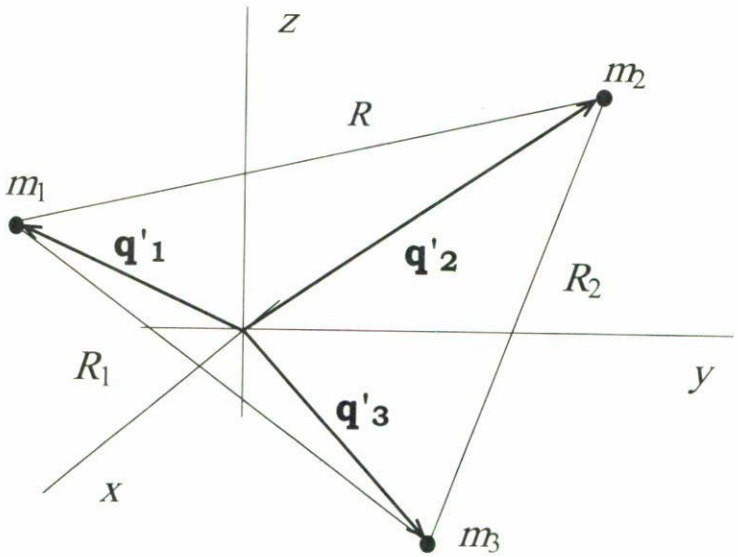

FIGURE 1. Geometry of the problem.

After introducing the geometry and notation of our problem, we shall sketch the necessary mathematical tools for integrating the equations of motion of the TBP, in a fashion that reliably handles the singularities associated to the Coulomb potential in binary collisions. We will then present some details concerning the program itself, and will finish with some results obtained with it on the helium atom and the positronium negative ion (Ps^-).

At this point it should perhaps be noted that, even though these are systems which in rigor should be treated quantum mechanically, theoretical developments from the last few decades have shown the relevance of a detailed knowledge of the *classical* behavior of non-integrable systems in the analysis of many purely quantum aspects (see Ref. [5], but also Refs. [3], [10]).

2. THE THREE BODY HAMILTONIAN

Let us then consider a system consisting of three point particles with masses m_i and charges Z_i $(i = 1, 2, 3)$ interacting through a Coulomb potential in free space. The coordinates and momenta of particle 1 will be described by the vectors $\mathbf{q}'_1 = (q'_1, q'_2, q'_3)$ and $\mathbf{p}'_1 = (p'_1, p'_2, p'_3)$, respectively, with analogous expressions —adjusting the indices accordingly— for the other two. The geometry of the problem is illustrated in Fig. 1, where the inter-particle distances R, R_1 and R_2 are indicated.

Since a system with all three charges of equal sign is of no physical interest when looking for bound states, we assume without loss of generality that particles 1 and 2 have charges $-Z_1$ and $-Z_2$, while particle 3 has charge $+Z_3$, with $Z_i > 0$ for $i = 1, 2, 3$. In atomic units,

and considering only Coulomb interactions, the Hamiltonian for this system is

$$H' = \sum_{r=1}^{3} \frac{\mathbf{p}_r'^2}{2m_r} - \frac{Z_1 Z_3}{R_1} - \frac{Z_2 Z_3}{R_2} + \frac{Z_1 Z_2}{R} \,. \tag{1}$$

The associated canonical equations of motion read

$$\frac{dq_r'}{dt} = \frac{\partial H'}{\partial p_r'}, \qquad \frac{dp_r'}{dt} = -\frac{\partial H'}{\partial q_r'} \qquad (r = 1, 2, ..., 9). \tag{2}$$

It is quite clear that the Hamiltonian from Eq. (1) is singular whenever any of the interparticle distances (R, R_1 or R_2) vanishes. From a strictly numerical standpoint, we will have problems when any of those distances becomes very small, even if it does not strictly vanish, since in Eq. (1) terms with very different magnitudes will have to be added.

3. REGULARIZATION PROCEDURE

One standard way of avoiding the problems associated to binary collisions in the Hamiltonian (1) —the three-particle collision cannot be regularized— was developed by Aarseth and Zare [1], based on previous work by Kustaanheimo and Steifel [7]. We will sketch here this procedure, whose detailed description can be found in Ref. [1], and more concisely in Ref. [15].

The basic idea is to obtain a canonical transformation which gives the Hamiltonian a non-singular form in the case of binary collisions, albeit at the expense of producing a set of dynamical equations significantly more complex in their algebraic expression. The resulting set of coordinates and momenta will be called regularized coordinates (Q, P).

3.1. Relative coordinates and extension of phase space

Briefly, in order to go from the (q', p') to the (Q, P) we first change to variables relative to m_3 with

$$\begin{aligned} \mathbf{q}_k &= \mathbf{q}_k' - \mathbf{q}_3', \qquad (k = 1, 2), \\ \mathbf{p}_k &= \mathbf{p}_k', \qquad (k = 1, 2), \\ \mathbf{q}_3 &= \mathbf{q}_3', \\ \mathbf{p}_3 &= \mathbf{p}_1' + \mathbf{p}_2' + \mathbf{p}_3'. \end{aligned} \tag{3}$$

We see from Eq. (3) that $\mathbf{p}_3$ is the total momentum of the system. We may then, without loss of generality, assume that in the original system (q', p') the center of mass is at rest, and we take it to be, for the sake of algebraic convenience, located at the origin. This eliminates six variables from our equations, and leaves us with a two-particle problem, which is however *not* further reducible to an equivalent one-particle description.

We next expand the dimension of the phase space by renaming variables according to

$$q_r \to q_{r+1}, \qquad p_r \to p_{r+1} \qquad (r = 4, 5, 6), \tag{4}$$

leaving the variables with $r \leq 3$ as before and defining the mock coordinates and momenta

$$q_4 \equiv 0, \qquad q_8 \equiv 0, \qquad p_4 \equiv 0, \qquad p_8 \equiv 0. \tag{5}$$

A discussion regarding the need for this extension can be found in Ref. [1].

3.2. Regularized coordinates and new time

We now introduce the regularized coordinates through a canonical transformation of the $(\mathbf{q}, \mathbf{p})$ to the $(\mathbf{Q}, \mathbf{P})$ associated to a generating function

$$W = W(\mathbf{p}, \mathbf{Q}) = \sum_{r=1}^{8} p_r f_r(\mathbf{Q}), \tag{6}$$

using the notation

$$\mathbf{p} = (p_1, p_2, p_3, p_4, p_5, p_6, p_7, p_8), \qquad \mathbf{Q} = (Q_1, Q_2, Q_3, Q_4, Q_5, Q_6, Q_7, Q_8). \tag{7}$$

The $f_r(\mathbf{Q})$, are continuous, differentiable functions yet unspecified, but which must obey the conditions

$$f_r = f_r(Q_1, Q_2, Q_3, Q_4) \qquad (r \leq 4), \tag{8}$$

$$f_r = f_r(Q_5, Q_6, Q_7, Q_8) \qquad (r > 4). \tag{9}$$

Let $\mathbf{A}$ be the matrix with components

$$A_{rs} = \frac{\partial f_s}{\partial Q_r}, \tag{10}$$

and $\mathbf{A}_1$, $\mathbf{A}_2$ its two non-zero blocks located on the diagonal.

If we assume the $f_r(\mathbf{Q})$ to be such that

$$\mathbf{A}_k \mathbf{A}_k^T = \lambda_k R_k \mathbf{I} \qquad (k = 1, 2), \tag{11}$$

where the λ_k are real numbers, $\mathbf{I}$ is the 4×4 identity matrix T represents matrix transposition, we can write our Hamiltonian as

$$\tilde{H}(\mathbf{Q}, \mathbf{P}) = \frac{\mathbf{P}_1^2}{2\mu_{13}\lambda_1 R_1} + \frac{\mathbf{P}_2^2}{2\mu_{23}\lambda_2 R_2} + \frac{\mathbf{P}_1^T \mathbf{A}_1 \mathbf{A}_2^T \mathbf{P}_2}{m_3 \lambda_1 \lambda_2 R_1 R_2} - \frac{Z_1 Z_3}{R_1} - \frac{Z_2 Z_3}{R_2} + \frac{Z_1 Z_2}{R}, \tag{12}$$

where

$$\mathbf{P}_1 = (P_1, P_2, P_3, P_4), \qquad \mathbf{P}_2 = (P_5, P_6, P_7, P_8). \tag{13}$$

Now, if in a system described by a time independent Hamiltonian H with parameter t, we include t as a coordinate and introduce a new time parameter τ, the new Hamiltonian H^* will be given by

$$H^* = (H - E)\frac{dt}{d\tau}, \tag{14}$$

being E the total energy of the system.

Therefore, by taking

$$dt = R_1 R_2 \, d\tau \tag{15}$$

we may avoid the divergences in Eq. (12) associated to $R_i \approx 0$, $i = 1, 2$.

In order for the regularization procedure to actually work we must now provide a set $\{f_r(\mathbf{Q})\}$ of functions which satisfies the requested conditions, Eqs. (8), (9) and (11). One such set is given by the Kustaanheimo-Steifel transformations, defined as

$$\begin{aligned} f_1 &= Q_1^2 - Q_2^2 - Q_3^2 + Q_4^2, & f_5 &= Q_5^2 - Q_6^2 - Q_7^2 + Q_8^2, \\ f_2 &= 2(Q_1 Q_2 - Q_3 Q_4), & f_6 &= 2(Q_5 Q_6 - Q_7 Q_8), \\ f_3 &= 2(Q_1 Q_3 + Q_2 Q_4), & f_7 &= 2(Q_5 Q_7 + Q_6 Q_8), \\ f_4 &= 0, & f_8 &= 0, \end{aligned} \tag{16}$$

which lead to condition (11) being valid with $\lambda_1 = \lambda_2 = 4$. The resulting regularized Hamiltonian is finally given by

$$\begin{aligned} \Gamma(\mathbf{Q}, \mathbf{P}) = {} & \frac{R_2}{8\mu_{13}}\mathbf{P}_1^2 + \frac{R_1}{8\mu_{23}}\mathbf{P}_2^2 + \frac{1}{16 m_3}\mathbf{P}_1^T \mathbf{A}_1 \mathbf{A}_2^T \mathbf{P}_2 \\ & - Z_3(R_1 Z_2 + R_2 Z_1) + R_1 R_2 \left(\frac{Z_1 Z_2}{R} - E\right), \end{aligned} \tag{17}$$

where the reduced masses with respect to m_3 are

$$\mu_{13} = \frac{m_1 m_3}{m_1 + m_3}, \qquad \mu_{23} = \frac{m_2 m_3}{m_2 + m_3}. \tag{18}$$

The canonical equations of motion associated to Eq. (17) are then

$$\frac{dQ_r}{d\tau} = \frac{\partial \Gamma}{\partial P_r}, \qquad \frac{dP_r}{d\tau} = -\frac{\partial \Gamma}{\partial Q_r} \qquad (r = 1, 2, \ldots, 8). \tag{19}$$

The explicit form of the above equations for the general three dimensional case is quite cumbersome, although easily obtained with a symbolic manipulation program (such as Maple or Mathematica). It is nonetheless useful to note that the derivatives $\partial R/\partial Q_i$ can be expressed in a compact form which is more efficient for numerical purposes than the one obtained by direct differentiation. By defining the 8×1 column vector $\mathbf{g}$ as

$$\mathbf{g} = \begin{bmatrix} \mathbf{f}_1 - \mathbf{f}_2 \\ \mathbf{f}_2 - \mathbf{f}_1 \end{bmatrix}, \tag{20}$$

where the vectors $\mathbf{f}_1$ and $\mathbf{f}_2$ are

$$\mathbf{f}_1 = \begin{bmatrix} Q_1^2 - Q_2^2 - Q_3^2 + Q_4^2 \\ 2(Q_1Q_2 - Q_3Q_4) \\ 2(Q_1Q_3 + Q_2Q_4) \\ 0 \end{bmatrix}, \qquad \mathbf{f}_2 = \begin{bmatrix} Q_5^2 - Q_6^2 - Q_7^2 + Q_8^2 \\ 2(Q_5Q_6 - Q_7Q_8) \\ 2(Q_5Q_7 + Q_6Q_8) \\ 0 \end{bmatrix}, \tag{21}$$

one can verify that the following relations hold [11]:

$$\frac{\partial R}{\partial Q_i} = \frac{1}{R}(\mathbf{Ag})_i, \qquad (i = 1, 2, \ldots, 8). \tag{22}$$

3.3. Transformation equations

The explicit expressions for the transformations to regularized coordinates, resulting from the above definitions, are

$$\begin{aligned} Q_1 &= \left[\tfrac{1}{2}(|\mathbf{q}_1| + q_1)\right]^{1/2}, & Q_2 &= q_2/2Q_1, \\ Q_3 &= q_3/2Q_1, & Q_4 &= 0, \end{aligned} \tag{23}$$

for $q_1 \geq 0$; or

$$\begin{aligned} Q_2 &= \left[\tfrac{1}{2}(|\mathbf{q}_1| - q_1)\right]^{1/2}, & Q_1 &= q_2/2Q_1, \\ Q_3 &= 0, & Q_4 &= q_3/2Q_2, \end{aligned} \tag{24}$$

for $q_1 < 0$. For the variables (Q_5, Q_6, Q_7, Q_8) we have analogous expressions, obtained by adding 4 to all indices and replacing $\mathbf{q}_1$ by $\mathbf{q}_2$.

The interparticle distances R_1, R_2 and R, expressed in terms of the regularized coordinates, can be cast in the form

$$R_1 = \sum_{r=1}^{4} Q_r^2, \qquad R_2 = \sum_{r=5}^{8} Q_r^2, \tag{25}$$

and

$$R^2 = R_1^2 + R_2^2 - 2\mathbf{f}_1 \cdot \mathbf{f}_2. \tag{26}$$

Finally, the regularized momenta are given by

$$\mathbf{P}_k = \mathbf{A}_k \mathbf{p}_k \qquad (k = 1, 2), \tag{27}$$

where

$$\mathbf{p}_1 = (p_1, p_2, p_3, p_4), \qquad \mathbf{p}_2 = (p_5, p_6, p_7, p_8). \tag{28}$$

4. CALCULATION PROGRAM

Through the time scale change, the effect of the regularization is to take very small time steps near the binary collisions ($R_1 \approx 0$ or $R_2 \approx 0$), while keeping a non-divergent Hamiltonian. However, despite this intrinsically adaptive nature of the regularized formulation, numerical work shows that if one wishes to balance efficiency and precision, it is necessary to implement an adaptive step size algorithm for the differential equation integrator.

Our program, developed in C++, uses a standard 4^{th} order Runge-Kutta adaptive step size integrator [12] driven by a routine which takes care of coordinate transformations, memory storage, disk swapping of data and Poincaré section calculations. In order to improve the accuracy of the results, Poincaré sections are obtained using reverse integration over the trajectory to find the intersection between the orbit and the Poincaré surface instead of interpolation, a method proposed by M. Hénon [6].

The program attempts to be useful for interactive exploration of the TBP, allowing control of the parameters which define the system and the integration conditions such as charges, masses, positions and momenta, error tolerance, etc. Initial conditions are defined in laboratory coordinates, integration is performed in the regularized ones, and position output data files are generated in center of mass coordinates for viewing convenience (to eliminate from the plots uniform displacements of the system). Besides position data, the program generates files with relative coordinates, Poincaré sections and a time-energy file which, since the system is conservative, serves as a checkout file for numerical problems. Langmuir type orbits [4] and Poincaré sections in hyperspherical coordinates can be obtained though menu options.

Since considerable simplification of the equations of motion and coordinate transformations results from assuming that the three particles evolve in a plane, the source code includes all the expressions corresponding to both the two and three dimensional cases. This allows the compilation of programs for both types of configurations, with fast integration of the plane cases and a slower but general option for three dimensional studies.

The resulting program, usable as a tool for numerical exploration of the general Coulomb TBP, produces accurate orbits in reasonable times on a typical desktop computer for most three dimensional configurations. Source code is available from the authors upon request.

Finally, we shall present some results obtained with the program for two typical three body systems, namely the Helium atom and the Positronium negative ion (*i.e.*, $e^- e^+ e^-$, abbreviated Ps^-).

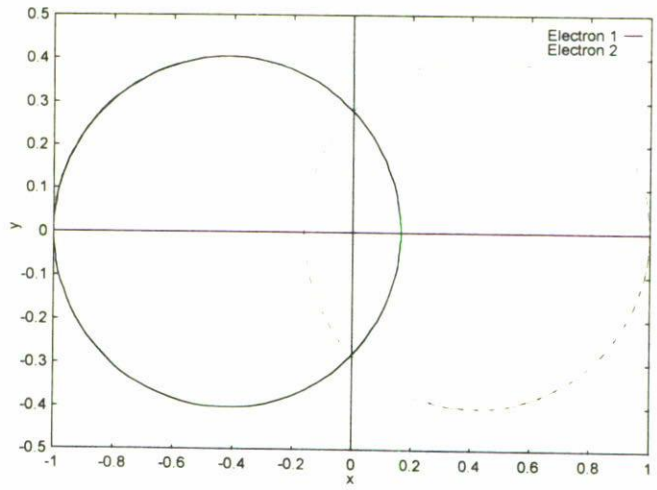

(a)

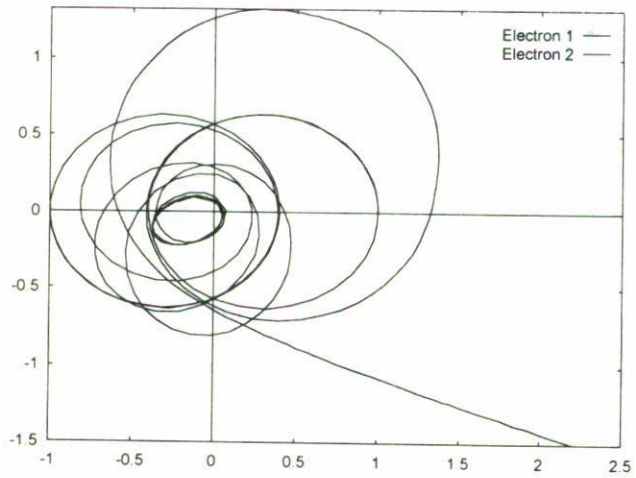

(b)

FIGURE 2. Wannier orbits in the He atom. (a) Typical orbit. (b) Slightly perturbed trajectory.

5. THE HELIUM ATOM

5.1. Wannier orbits

In the so-called Wannier configuration, both electrons orbit around the nucleus with equal angular momentum, satisfying

$$\mathbf{r}_1(t) = -\mathbf{r}_2(t). \tag{29}$$

In can be shown [15], that this condition leads to elliptic trajectories. This type of orbit was proposed as one of the first classical models for the Helium atom, but the presence of a diverging Lyapunov exponent leads to expect it to be of little significance as a realistic description of this system. Quantum calculations confirm this prediction (see Ref. [15] for

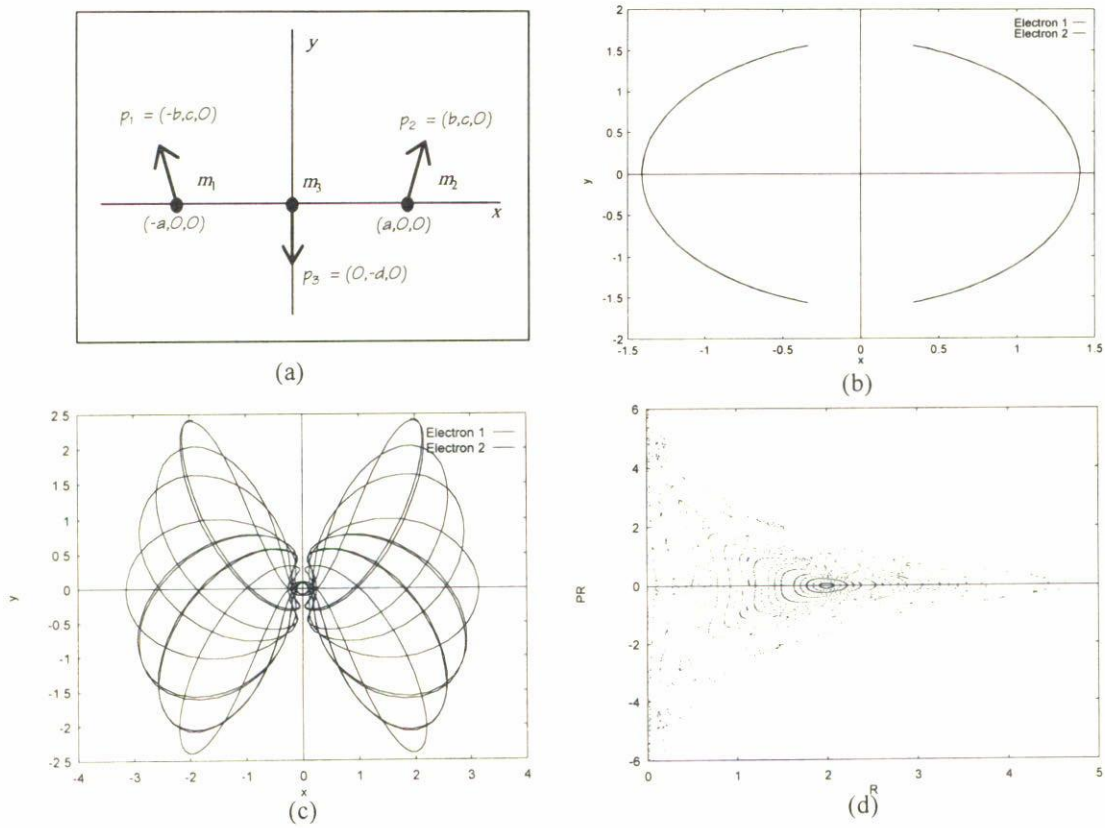

FIGURE 3. Langmuir type orbits in the He atom. (a) Geometry of the initial conditions. (b) Basic orbit (shortest periodic orbit in the He atom). (c) A more complex orbit. (d) Poincaré map of a family of trajectories in hyperspherical coordinates ($R - P_R$ plot).

a discussion), which can be also checked numerically by performing slight variations in the initial conditions. Fig. 2a shows a typical Wannier orbit, and in Fig. 2b we have a horizontal displacement of 10^{-4} in the initial position of one electron, leading rapidly to ionization. This suggests that the orbit is unstable, as other types of perturbations to the initial conditions confirm.

5.2. Langmuir type orbits

This is another classical model for the He atom, which exhibits the shortest periodic orbit of this system [see Fig. 3b], an orbit surrounded by a stability island in phase space. Although strictly speaking the Langmuir orbit is the one just mentioned, one can study the family of orbits whose initial condition exhibit the symmetry shown in Fig. 3a. Our program can generate orbits of this type asking for the values of a, b and the total energy E: those shown in Figs. 3b and 3c are obtained with $a = 1.40706$ and $a = 0.25$, respectively ($E = -1$, $b = 0$ for both).

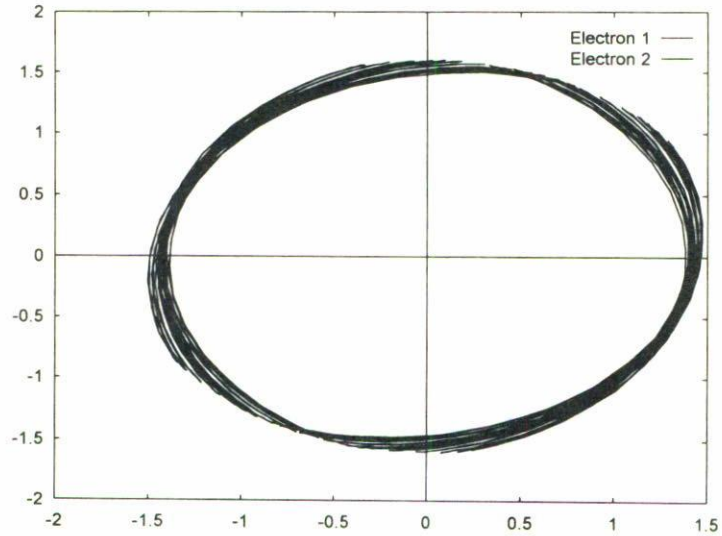

(a)

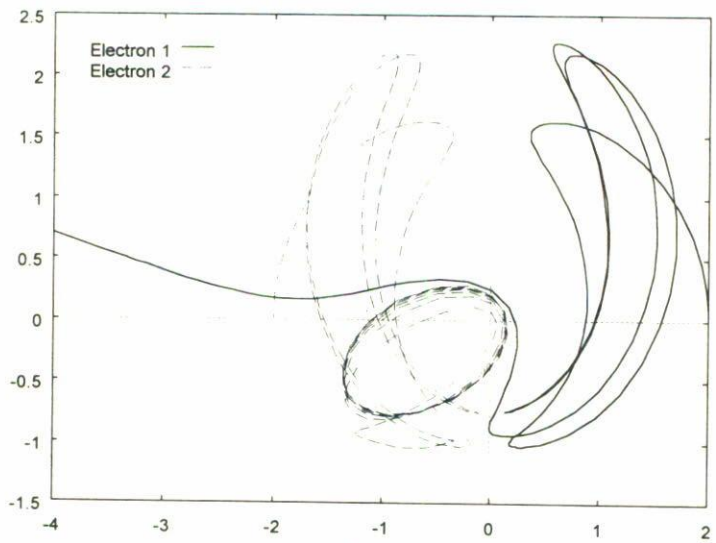

(b)

FIGURE 4. Perturbations on Langmuir type orbits.

The stability of these orbits in phase space can be easily seen by making a Poincaré map in terms of the hyperspherical radius R defined as

$$R = \sqrt{|\mathbf{r}_1|^2 + |\mathbf{r}_2|^2} \tag{30}$$

and its associated canonical momentum p_R [8]. Such a map (with $E = -1$, $b = 0$ for 28 orbits varying a from 0.05 to 1.4) is shown in Fig. 3d where the "basic" orbit from Fig. 3a appears as a dot at $R = 1.98988$ (*i.e.*, $a = 1.40706$).

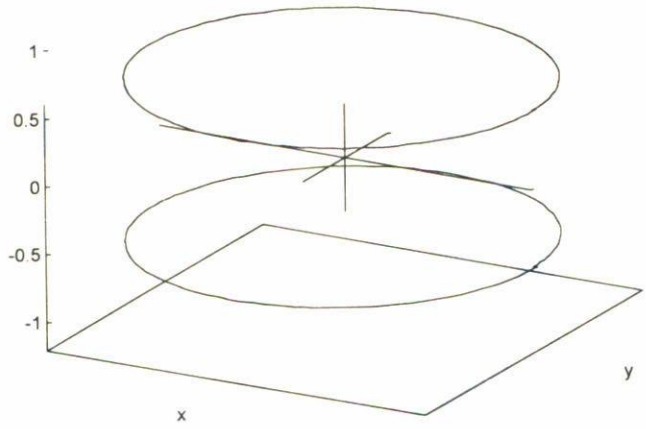

(a)

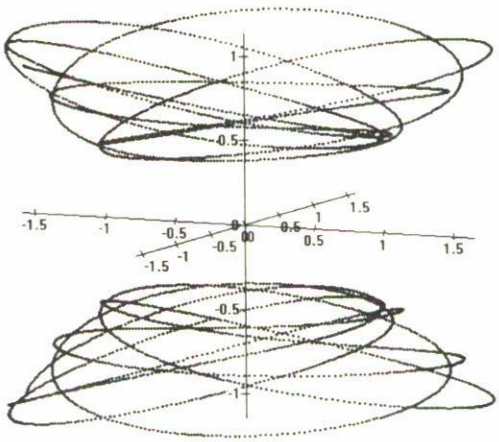

(b)

FIGURE 5. Asymmetric top orbits in the He atom.

Now, numerical testing with perturbations on the initial conditions which alter the symmetry of the configuration shows that the "basic" orbit is stabler than more complex ones. Figures 4a and 4b were respectively obtained with $a = 1.40706$, $b = 0$, $E = -1$ and $a = 2$, $b = 0$, $E = -1$ as starting points, introducing then a change in the x-coordinate of *one* electron of magnitude $\delta x = 10^{-3}$ in the first case and $\delta x = 10^{-6}$ in the second. In Fig. 4a no ionization occurs with an integration time of $t = 100$ (atomic units), while Fig. 4b shows auto-ionization after $t = 45$.

This result agrees with what can be inferred from the Poincaré map just discussed, for the basic orbit is surrounded by a sharply defined torus structure which we expect to exist in phase space even when the symmetry of the configuration is slightly broken, while such a structure does not exist for orbits around $a = 2$ (*i.e.*, $R = 4$).

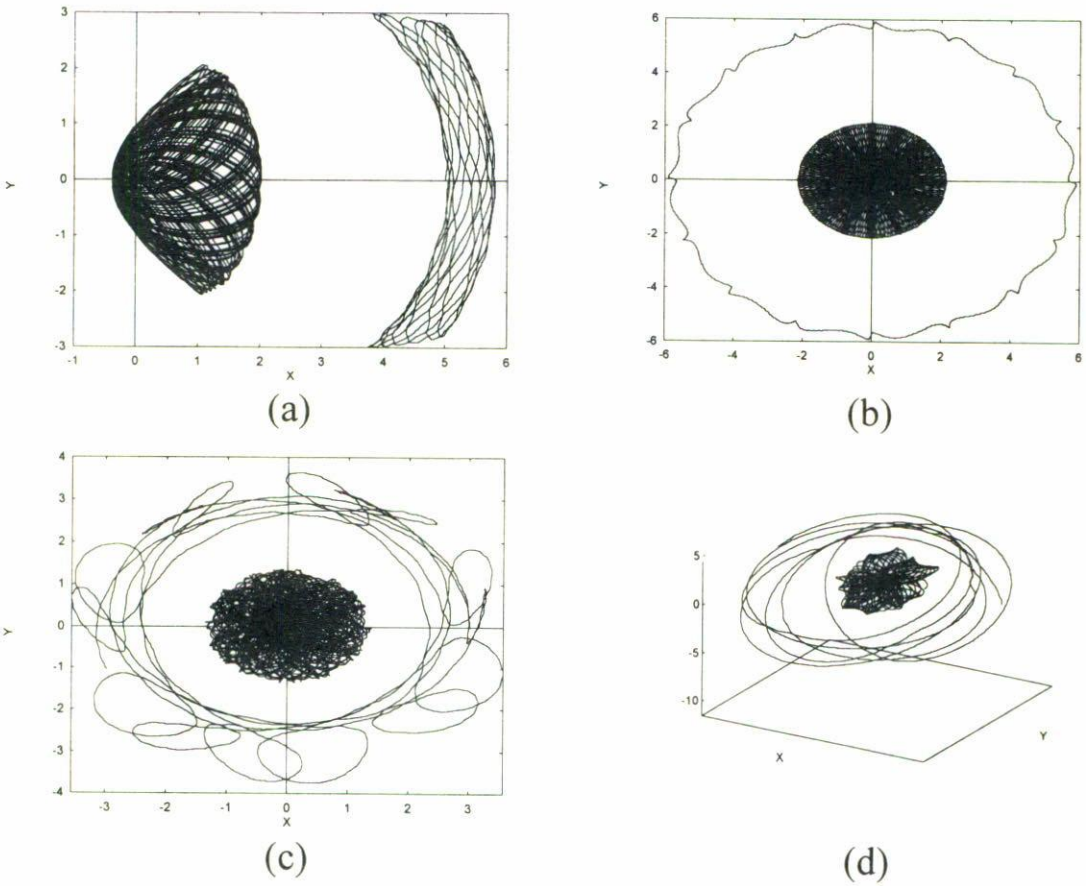

FIGURE 6. Planetary configurations for the He atom. (a) Variation on the frozen planet, $L = 0$. (b) Periodic orbit with $L \neq 0$. (c) Orbit where the electrons are closer, and therefore may have a stronger interaction. (d) Three-dimensional configuration.

5.3. Asymmetric top

This is another model originally proposed by Langmuir for the He atom, where the electrons form an equilateral triangle which rotates riddidly around the nucleus. The trajectory is shown in Fig. 5a, resulting from the initial conditions $\mathbf{r}_1 = (\sqrt{3}/2, 0, 1/2)$, $\mathbf{r}_2 = (\sqrt{3}/2, 0, -1/2)$, $\mathbf{p}_1 = \mathbf{p}_2 = (0, p_0, 0)$, with $p_0 = 1.225$. If these exact conditions are not given but the basic symmetry is maintained, non-ionizing orbits can be obtained, such as the one from Fig. 5b, which has $p_0 = 1.4$.

5.4. Planetary configuration

This name is given to geometries where on the average $R_1 \gg R_2$. They possess both experimental and theoretical interest [13, 14], and can exist in various different forms.

If $L = 0$ (L is the total angular momentum), we obtain a family of configurations where the simplest one is the so called "frozen planet" [13]: one electron oscillates near the nucleus

and the other remains almost stationary further away. Slightly different conditions which respect $L = 0$ produce orbits like the one in Fig. 6a, while for $L \neq 0$ both electrons can evolve in complete revolutions around the nucleus, albeit with very different frequencies: Fig. 6b displays one such trajectory.

If the electrons are allowed to interact more (by not satisfying $R_1 \gg R_2$ so rigidly), this interaction can produce significant deformations on the orbits, but they may still exist for long periods: Fig. 6c was obtained with initial conditions $\mathbf{r}_1 = (1,0,0)$, $\mathbf{r}_2 = (3,0,0)$, $\mathbf{p}_1 = (0,-1,0)$, $\mathbf{p}_2 = (0,0.4,0)$ and an integration time of $t = 601$ (for a discussion, see [18]).

Finally, three-dimensional planetary configurations are also possible, such as the one in Fig. 6d.

6. THE Ps^- ION

6.1. Langmuir orbits

Wannier orbits in the Ps^- ion exist identical to those in the He atom (symmetry maintains the e^+ static in the center), and hence will not be shown.

Langmuir type orbits, with the same geometry form Fig. 3a also exist in the Ps^- ion, although here the e^+ oscillates in a vertical straight line (plots are in the center of mass system). In the Ps^-, the simplest orbit has a more complex geometry than in the case of He, as shown in Fig. 7a, caused by the motion of the e^+ just mentioned. Here we also have a whole family of trajectories, whose typical aspect is that of Fig. 7a.

The absence of an orbit as simple as in Helium is clear in the Poincaré section in hyperspherical coordinates shown in Fig. 7c: there is a "hole" in the center of the map, around which the simplest orbit (Fig. 7a) winds itself. This map seems at first sight chaotic, but this is just a visual effect, as can be seen by plotting only a few trajectories (Fig. 7d); a chaotic behavior would lead to these few orbits densely filling the entire region (or at least some subregions) instead of just tracing finite sets of points.

Langmuir orbits in Ps^- show even more sensitiveness to perturbations which destroy the symmetry of the configuration than in Helium, as can be easily checked numerically. Here, even the simplest configuration ionizes rapidly if its initial conditions are not exactly symmetrical.

We must note that for three particle systems with finite masses, it is standard [2] to use a different definition for hyperspherical coordinates than the one given for He. Although expression (30) remains valid for the hyperradius R, and its associated canonical momentum p_R is constructed in the usual fashion, the vectors $\mathbf{r}_1$ and $\mathbf{r}_2$ are now defined as [2]

$$\mathbf{r}_1 = \mathbf{q}_2 - \mathbf{q}_1, \tag{31}$$

$$\mathbf{r}_2 = \sqrt{\frac{\mu_{12,3}}{\mu_{12}}}\left[-\frac{1}{2}(\mathbf{q}_1 + \mathbf{q}_2) + \mathbf{q}_3\right], \tag{32}$$

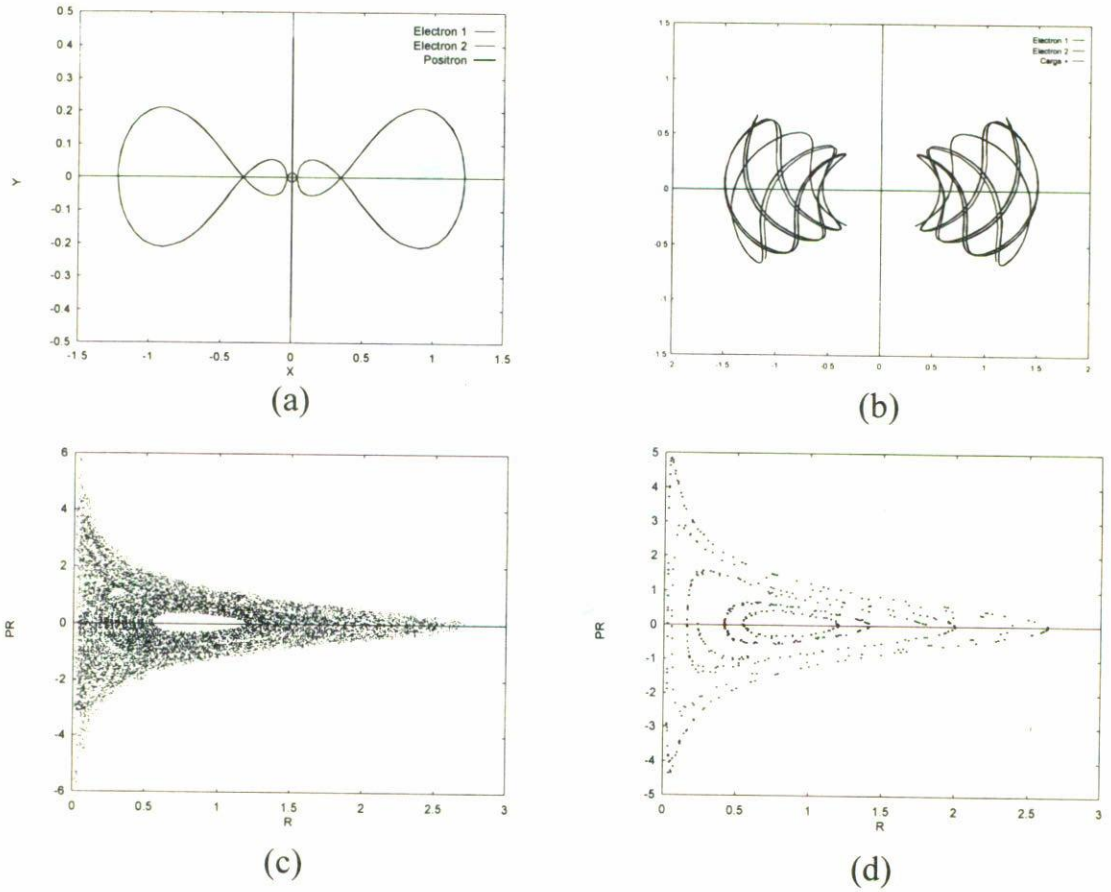

FIGURE 7. Langmuir type orbits in the Ps^- ion. (a) Shortest periodic orbit. (b) A more complex one. (c) Poincaré map. (d) Detail of the Poincaré map showing the regular structure of the orbits.

where

$$\mu_{12,3} = \frac{(m_1 + m_2)m_3}{m_1 + m_2 + m_3}, \qquad \mu_{12} = \frac{m_1 m_2}{m_1 + m_2}, \tag{33}$$

and $\mathbf{q}_1$, $\mathbf{q}_2$ and $\mathbf{q}_3$ are the position vectors of particles 1, 2 and 3, respectively, in the center of mass system.

6.2. Asymmetric top

The basic definitions are in this case the same as for Helium, and we also have non-ionizing orbits, although very sensitive to symmetry-breaking changes in the initial conditions [see Fig. 8].

6.3. Planetary configurations

Through numerical search, no bound planetary configurations were found for the Ps^- ion, with all attempts resulting in orbits like Fig. 9a. A plausible hypothesis for this

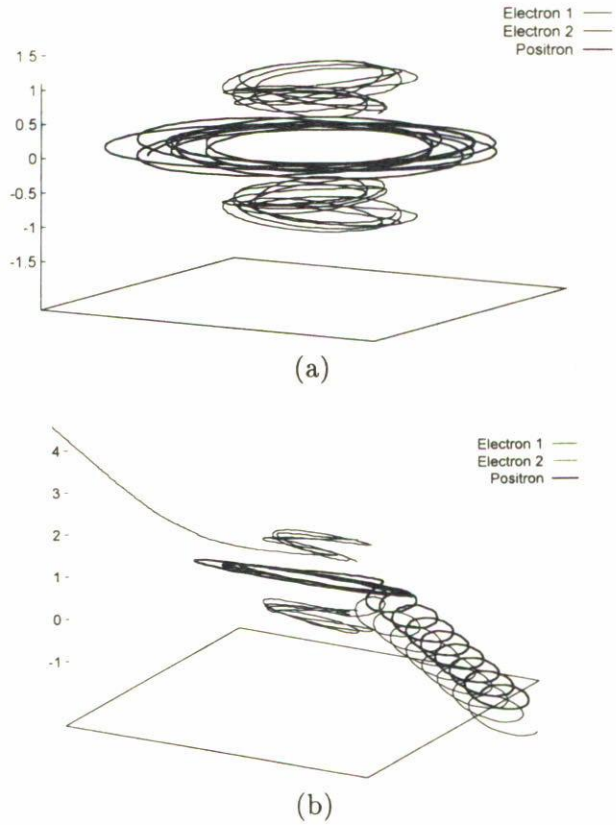

FIGURE 8. Asymmetric top orbits for the Ps^- ion. (a) One such orbit. (b) Symmetry-breaking perturbation on the initial conditions, rapidly leading to autoionization.

phenomenon is that, since in Ps^- the positive particle has charge $+1$, the outer electron sees a zero mean field from the e^-e^+ pair, too weak to keep it bound. In order to test the validity of this statement, we gave the positive particle a charge $+2$, keeping all other parameters equal: the resulting orbit, shown in Fig. 9b, is bound.

7. CONCLUSIONS

A general program for the numerical integration of the classical Coulomb three body problem was presented, which uses regularized coordinates in order to obtain reliable results even in the case of close inter-particle encounters. The program, written in C++, permits interactive changes to all system parameters.

In the Helium atom, we studied numerically the Wannier, Langmuir —oscillatory and asymmetric top— and planetary configurations. Except for the last one, these are all geometries with special symmetries, and we found them in general to be extremely sensitive to changes in the initial conditions which disrupted such symmetries.

Planetary configurations, not associated to any specific geometrical symmetry, were found to be more robust with respect to variations in the initial conditions. This suggests

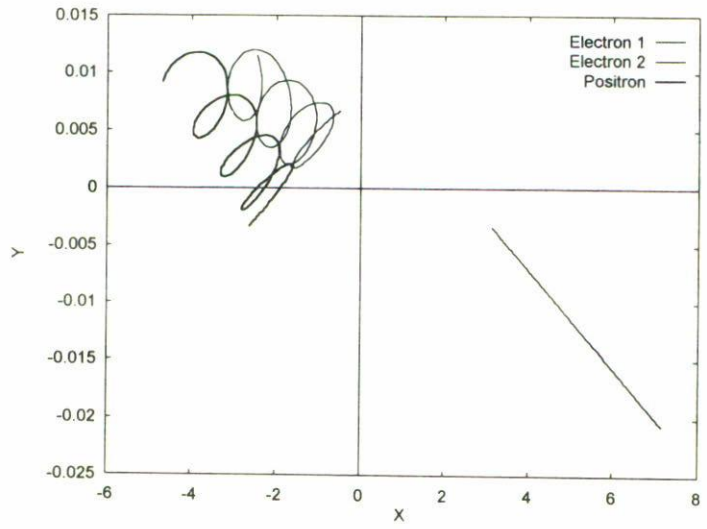

(a)

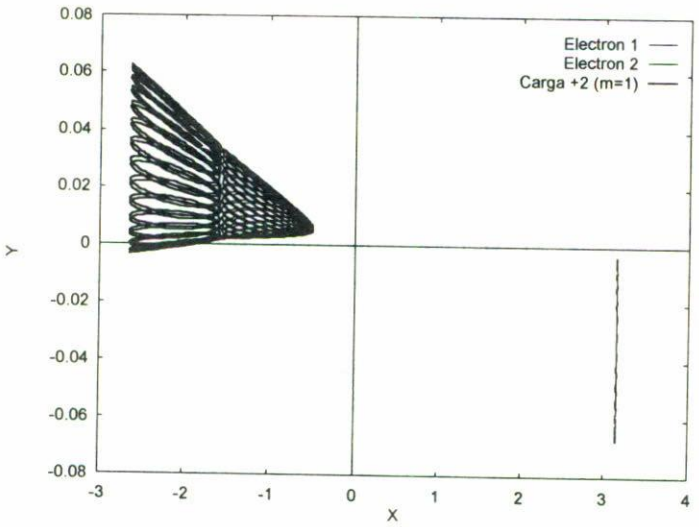

(b)

FIGURE 9. Planetary configurations. (a) Ps^- ion: no stable ones were found. (b) Hypothetical system with charge $2e^+$ at the nucleus leads to non-ionizing orbits.

that they may occupy, with non-ionizing orbits, a larger region in phase space than do the aforementioned configurations. Since both periodic and quasi-periodic orbits were found, and because of their significance in phase space, they appear as important geometries for a semi-classical quantization of certain states of the He atom, especially doubly excited states with appreciably different quantum numbers for both electrons.

With the Ps^- ion, we found results analogous to those of helium, concerning the sensitivity of all configurations with respect to the symmetry in the initial conditions. However, the Ps^- ion appears numerically to be unstabler than helium, with shorter self-ionization

times and no bound planetary configurations: only the strictly symmetrical models lead to classically bound states. This can be regarded as a classical justification for the experimentally observed instability of the Ps^- ion [9].

Finally, the program was recently used to confirm through numerical experiments, theoretical predictions concerning special geometries in Coulomb three body systems [16, 17].

ACKNOWLEDGMENTS

We would like to thank Dr. Manuel Páez for very helpful discussions regarding computing aspects of the problem. Support from Colciencias and CIEN, under contract N° 1115–05–012–92, is gratefully acknowledged.

REFERENCES

1. S.J. Aarseth and K. Zare, *Celest. Mech.* **10** (1974) 185.
2. J. Botero, *Phys. Rev.* **A35** (1987) 36.
3. D. Delande and A. Buchleitner, *Adv. At. Mol. Opt. Phys.* **34** (1994) 85.
4. M.S. Dimitrijević and P.V. Grujić, *Z. Naturforsch.* **39a** (1984) 930.
5. M.C. Gutzwiller, *Chaos in Classical and Quantum Mechanics*, Springer, Berlín (1990).
6. M. Hénon, *Physica* **5D** (1982) 412.
7. P. Kustaanheimo and E. Steifel, *J. Reine Angew. Math.* **218** (1965) 204.
8. J. Mahecha, *J. Phys. B: At. Mol. Opt. Phys.* **27** (1994) 1925.
9. A.P. Mills, *Phys. Rev. Lett.* **50** (1983) 671.
10. M. Nauenberg, *Comments At. Mol. Phys.* **25** (1990) 151.
11. F. Pérez, 1994. Undergraduate thesis, Universidad de Antioquia, Departamento de Física (Unpublished).
12. W.H. Press, S.A. Teukolsky, W.T. Vetterling and B.P. Flannery, *Numerical Recipes in C*, Cambridge, Cambridge University Press (1988).
13. K. Richter and D. Wintgen, *Phys. Rev. Lett.* **65** (1990) 1965.
14. K. Richter and D. Wintgen, *J. Phys. B: At. Mol. Opt. Phys.* **24** (1991) L565.
15. K. Richter, G. Tanner and D. Wintgen, *Phys. Rev.* **A48** (1993) 4182.
16. A. Santander, 1995. Undergraduate thesis, Universidad de Antioquia, Departamento de Física (Unpublished).
17. A. Santander, J. Mahecha and F. Pérez, "Rigid rotor and fixed shape solutions in the Coulombic three body problem", *Few Body Systems* (presented for publication).
18. T. Yamamoto and K. Kaneko, *Phys. Rev. Lett.* **70** (1993) 1928.